Tetrahedron 70 (2014) 3553–3559

Contents lists available at ScienceDirect

Tetrahedron

journal homepage: www.elsevier.com/locate/tet

Facile preparation of water dispersible red fluorescent organic nanoparticles and their cell imaging applications

Xiqi Zhang *,†, Xiaoyong Zhang †, Bin Yang, Yaling Zhang, Yen Wei *

Department of Chemistry and the Tsinghua Center for Frontier Polymer Research, Tsinghua University, Beijing 100084, China

ARTICLE INFO

Article history:
Received 29 January 2014
Received in revised form 29 March 2014
Accepted 3 April 2014
Available online 12 April 2014

Keywords:
Red fluorescent organic nanoparticles
Tetraphenylethene
Lecithin
Surfactant modification
Cell imaging

ABSTRACT

Red fluorescent organic nanoparticles (FONs) based on a cyano-substituted diarylethylene and tetraphenylethene derivative conjugated molecule (**R-TPE**) were facilely prepared via surfactant modification with lecithin for the first time. The obtained **R-TPE-LEC** FONs were characterized by a series of techniques including fluorescence and UV spectroscopy, Fourier transform infrared spectroscopy, and transmission electron microscopy. Biocompatibility evaluation and cell uptake behavior of **R-TPE-LEC** FONs were further investigated to explore their potential biomedical application. We demonstrated that such red FONs exhibit anti-aggregation-caused quenching property, broad excitation wavelength, high water dispersibility, uniform morphology (40–60 nm), and excellent biocompatibility, making them promising for cell imaging application.

1. Introduction

Optical bioimaging is one of the rapid growing areas in biological and biomedical research.[1] Fluorescence cellular probes with red/near-infrared (R/NIR, >600 nm) emission are highly desirable for biological applications due to their low optical absorption and autofluorescence of biological media.[2–5] Up to date, various fluorescent materials including organic dyes,[6] fluorescent proteins,[7] fluorescent inorganic nanoparticles (NPs)[8–13] have been used as R/NIR probes. However, many of these fluorescent materials often suffer from obvious disadvantages, such as water insolubility, photobleaching, and toxicity, which severely limited their practical bioimaging applications. For example, most of organic dyes are intrinsic hydrophobic and instable in biological media.[14] Usage of fluorescent proteins is often limited due to the high cost, low molar absorptivity, and low photobleaching thresholds.[15] While inorganic NPs or quantum dots are non-biodegradable and often toxic to living organisms.[16–19] Compared with the current used fluorescent bioprobes, fluorescent organic nanoparticles (FONs) have recently received more and more attentions due to flexible synthetic approaches of these small organic molecules and their biodegradation potential.[20–25] Because of these virtues, various FONs including fluorescent conjugated polymers, polydopamine nanoparticles, and aggregation-induced-emission (AIE) or aggregation induced emission enhancement (AIEE) materials based FONs have been reported in recent years.[26–37] Among them, the AIE or AIEE based FONs have attracted great research interest because they could overcome the notorious aggregation-caused quenching (ACQ) effect of most organic dyes. Different AIE or AIEE units, such as siloles,[38] diphenylacrylonitrile,[39–43] tetraphenylethene,[44–48] triphenylethene,[49–54] distyrylanthracene derivatives[55–59] conjugated molecules have been examined for chemosensors and bioimaging applications.

However, direct using of AIE or AIEE based FONs for bioimaging has been proven problematic due to the strong hydrophobicity of most of AIE or AIEE units. The introduction of charges into AIE (or AIEE) materials could improve their solubility in aqueous media, but the electric charges of the highly concentrated ionized dyes may affect intracellular physiology and sometimes even kill the cells.[52] Therefore, facile preparation of novel FONs, which exhibited enhanced water dispersibility, excellent biocompatibility, and photoluminescent properties simultaneously is of great significance.

In our recent report, we have demonstrated that hydrophobic AIE unit (**An18**) could be facilely transferred into hydrophilic FONs via mixing of **An18** and a commercial surfactant pluronic F127.[30] The **An18** based FONs showed good water solubility and excellent biocompatibility are promising for cell imaging applications. However, one of the disadvantages of these AIE-based FONs for

* Corresponding authors. Tel.: +86 10 6279 2604; e-mail addresses: sychyzhang@126.com (X. Zhang), weiyen@tsinghua.edu.cn (Y. Wei).
† These authors contributed equally to this work.

0040-4020/$ – see front matter © 2014 Elsevier Ltd. All rights reserved.
http://dx.doi.org/10.1016/j.tet.2014.04.010

bioimaging applications is that their maximum emission wavelength is not long enough (filled into 530–550 nm), which will inevitably interfered by the body optical absorption, light scattering, and autofluorescence of biological media.

Herein, we report a facile method for the preparation of red FONs based on a cyano-substituted diarylethylene and tetraphenylethene derivative (**R-TPE**) (derivatized from 4,8-bis[5-(2-ethylhexyl)-2-thienyl]benzodithiophene core structure with bis [2-(tetraphenylethene)-acrylonitrile] side groups, its synthetic route was shown in Scheme 1) by surfactant modification of lecithin (Scheme 2). **R-TPE** was firstly dissolved in THF, mixed with the aqueous solution of surfactant lecithin by sonication. With the removal of THF, the red FONs **R-TPE-LEC** formed. The hydrophobic surface of **R-TPE** was changed to hydrophilic by surrounding with lecithin, thus the **R-TPE-LEC** FONs exhibit good water dispersibility and anti-ACQ property. To exploit the potential biomedical applications of such red FONs, their biocompatibility as well as cell imaging applications were further investigated.

2. Results and discussion

2.1. Characterization of R-TPE-LEC FONs

2.1.1. Fluorescence spectra. The fluorogen **R-TPE** was prepared following the synthetic route shown in Scheme 2 (see Experimental procedure). Its structure was characterized and confirmed by standard spectroscopic methods. The fluorescent dye **R-TPE** is hydrophobic and emits strong crimson fluorescence in solid state. When **R-TPE** is dissolved in DMSO, it has strong orange fluorescence in dispersed state. After modified by surfactant lecithin, **R-TPE** could be dispersed well in water by the hydrophobic interaction of lecithin, meanwhile, the fluorogen is still in aggregated state in the **R-TPE-LEC** nanoparticles, and the **R-TPE-LEC** composite emitted strong red fluorescence (612 nm for the maximum emission wavelength) in water with almost the same fluorescent intensity like that in a pure DMSO solution (Fig. 1(A)), which show obvious anti-ACQ property. Meanwhile, fluorescence quantum

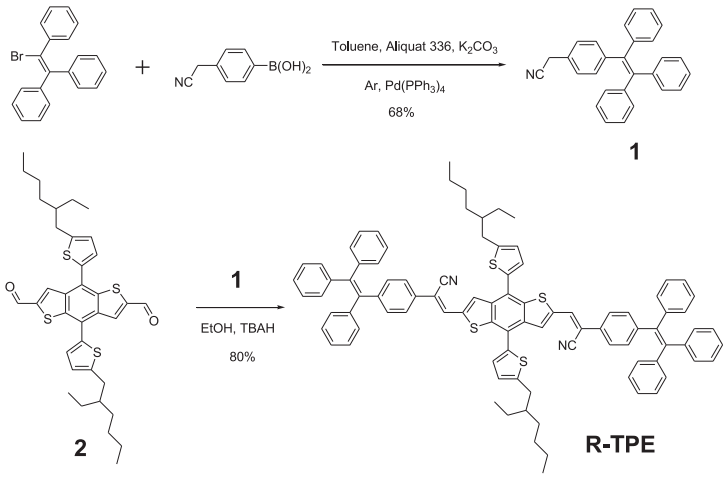

Scheme 1. Synthetic route of **R-TPE**.

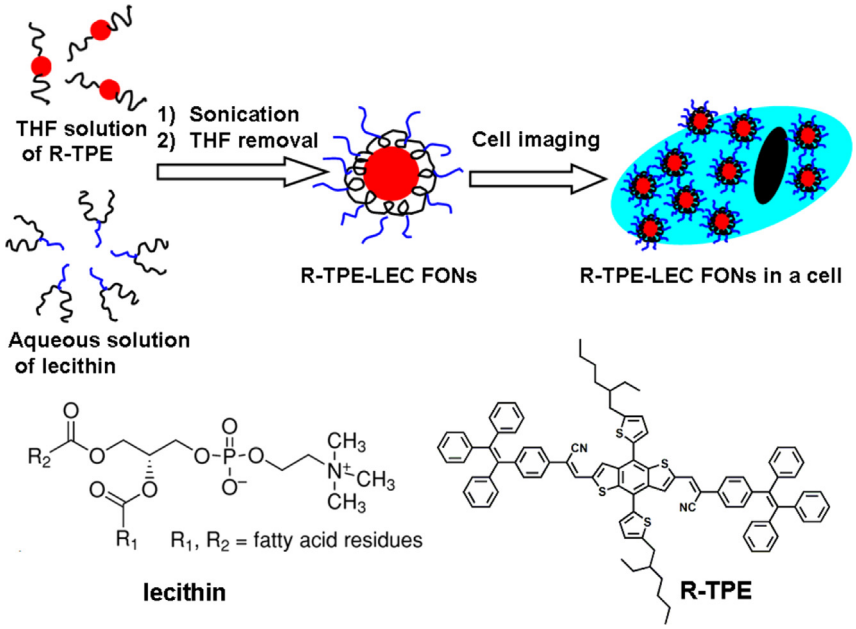

Scheme 2. Schematic showing transformation of **R-TPE** from hydrophobic to hydrophilic red **R-TPE-LEC** FONs with lecithin and their use as cell imaging probes.

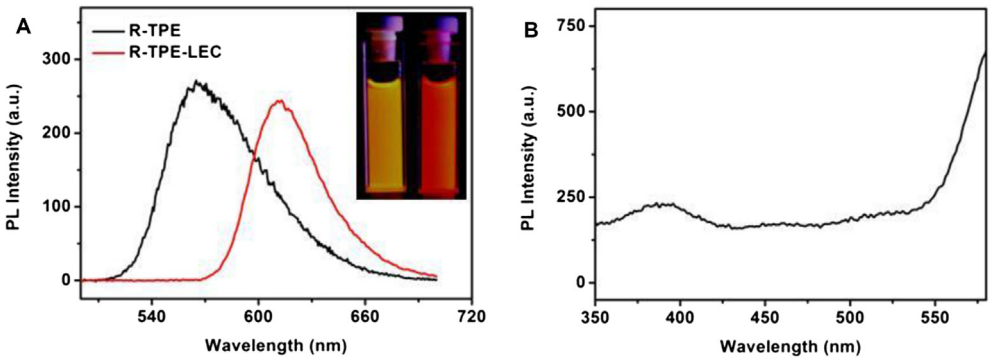

Fig. 1. (A) Fluorescence emission spectra of **R-TPE** in DMSO and surfactant modificated nanoparticles (**R-TPE-LEC**) dispersed in water. Inset: fluorescent image of **R-TPE** in DMSO and **R-TPE-LEC** in water taken at 365 nm UV light; (B) fluorescence excitation spectrum of **R-TPE-LEC** FONs in water.

yields (Φ_F) of **R-TPE** in DMSO and **R-TPE-LEC** FONs in water were estimated using Rhodamine 6G in ethanol as standard (Φ_F=95%), the absorbance of the solutions was kept around 0.05 to avoid internal filter effect. We demonstrated that the Φ_F of **R-TPE** in DMSO and **R-TPE-LEC** FONs in water were about 10.3% and 8.7%, respectively. When the nanoparticles formed, the fluorescent wavelength of the fluorescence dye emerged a 46 nm red-shifted emission than that of **R-TPE** in DMSO. The observed spectral shift is attributed presumably to the torsion-locking planarization of the distorted solution geometry of **R-TPE** by aggregation, which narrows the optical bandgap by lengthening the effective π-electron conjugation.[56] The appearance of a longer-wavelength emission also suggests that close stacking of the planarized **R-TPE** molecules is possibly accompanied with enhancing fluorescence J-type π-aggregation, often occurring in diarylacrylonitrile derivatives.[23,27] As shown in Fig. 1(B), the fluorescence excitation spectrum of **R-TPE-LEC** FONs in water exhibited broad excitation wavelength from 350 nm to 580 nm. It is noteworthy that when the excitation wavelength exceeds 540 nm, the fluorescence excitation intensity of such red FONs even significantly continuous increase with almost 3-fold as the wavelength reaches 580 nm. This excellent feature is greatly benefited for their potential cell imaging applications.

2.1.2. UV spectrum and TEM. As shown in the inset of Fig. 2(A), after surface modification with surfactant lecithin, the surfactant modificated nanoparticles **R-TPE-LEC** were readily dispersed in water, suggesting the successful formation of hydrophilic conjugated FONs. The UV absorption spectrum of **R-TPE-LEC** FONs in water showed that the maximum absorption wavelength located at 434 nm (Fig. 2(A)). The absorption spectrum of the FONs was not consistent with the excitation spectrum, and this phenomenon often could be seen in the FONs system, which might be due to the light scattering effect.[60–62] The UV absorption spectrum of **R-TPE** dissolved in DMSO was shown in Fig. 2(B) for comparison. The transmission electron microscopy (TEM) images further confirmed the formation of the conjugated FONs. Some small organic spheres with diameters ranging from 40 to 60 nm, which derived from the assembly of **R-TPE** and lecithin were observed (Fig. 2(C)). The formation of such nanostructures is likely due to the strong interactions between the alkyl chain of **R-TPE** and the hydrophobic segments of lecithin, meanwhile, the hydrophilic segments of lecithin were covered on the spheres to render them water dispersible. The size distribution of **R-TPE-LEC** FONs in water was also determined using a zeta Plus particle size analyzer. Results showed that the size distribution of **R-TPE-LEC** FONs in pure water was 170.7±3.8 nm with narrow polydispersity index (0.214). As compared with the size distribution in pure water, the size of the FONs characterized by TEM was significantly smaller likely due to shrinkage of micelle during the drying process. Taken together, due to excellent water solubility, uniform morphology, biodegradable potential, and unique photoluminescent (PL) properties (including anti-ACQ, broad excitation wavelength and long emission wavelength), we expect that **R-TPE-LEC** FONs can be potentially used for bioimaging applications.

2.1.3. FT-IR spectra. Furthermore, successful formation of **R-TPE-LEC** FONs was confirmed by FT-IR spectroscopy. As shown in Fig. 3, the peak located at 1746 cm^{-1} can be ascribed to the C=O stretching vibration band of ester bond in lecithin, and another peak located at 1073 cm^{-1} can be assigned to the bending vibration band of C–O in lecithin. As compared with **R-TPE**, lecithin, and **R-TPE-LEC** FONs, these two characteristic peaks located at 1746 cm^{-1} and 1073 cm^{-1} can be clearly observed in **R-TPE-LEC** FONs, demonstrating the successful modification of lecithin with **R-TPE**.

2.2. Biocompatibility of R-TPE-LEC FONs

To test the potential biomedical applications of **R-TPE-LEC** FONs, their biocompatibility with A549 cells were subsequently

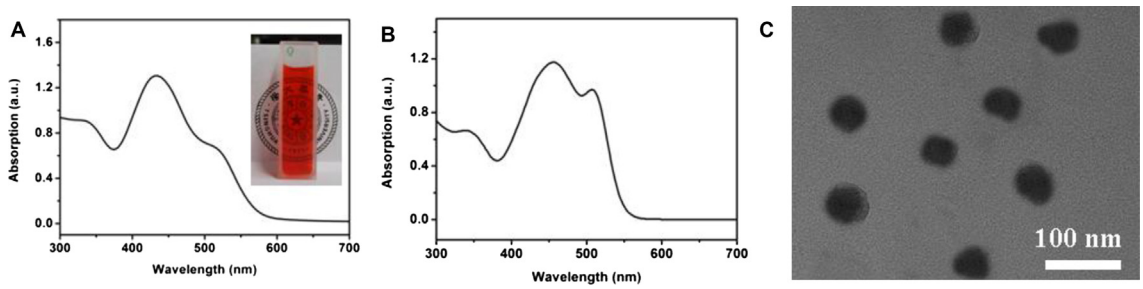

Fig. 2. (A) UV absorption spectrum of **R-TPE-LEC** FONs dispersed in water. Inset: visible image of **R-TPE-LEC** FONs in water using the logo of 'Tsinghua University' as background; (B) UV absorption spectrum of **R-TPE** dissolved in DMSO; (C) TEM image of **R-TPE-LEC** FONs dispersed in water, scale bar=100 nm.

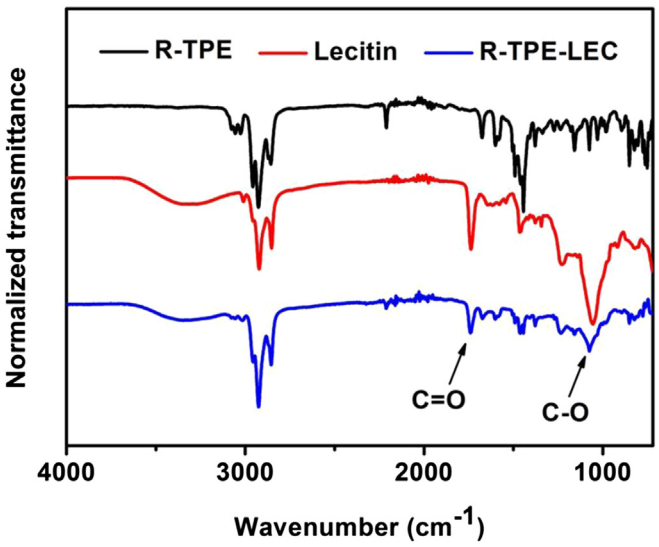

Fig. 3. FT-IR spectra of **R-TPE**, lecithin, and **R-TPE-LEC** FONs.

examined. Fig. 4(A)–(C) shows the microscopy images of cells when they incubated with different concentrations of **R-TPE-LEC** FONs for 24 h, and no significant cell morphology changes were observed. It can be seen that cells still attached very well to cell plate even the concentration of **R-TPE-LEC** FONs was up to 120 μg mL^{-1}. The optical microscopy images implied the good biocompatibility of **R-TPE-LEC** FONs. Cell viability of **R-TPE-LEC** FONs was further determined to quantitatively evaluate the biocompatibility of **R-TPE-LEC** FONs.[63] As shown in Fig. 4(D), no obvious cell viability decrease was found when cells were incubated with 40 μg mL^{-1} of **R-TPE-LEC** FONs for 8 and 24 h. The cell viability values were about 90% even the concentrations increased to 120 μg mL^{-1}, further confirming the excellent biocompatibility of **R-TPE-LEC** FONs.

2.3. Cell imaging applications of R-TPE-LEC FONs

The cell imaging applications of **R-TPE-LEC** FONs were further explored. The confocal laser scanning microscope (CLSM) images of cells incubated with 100 μg mL^{-1} of **R-TPE-LEC** FONs for 3 h were shown in Fig. 5. Bright field images (Fig. 5(A)) indicated that cells still kept their normal morphology, further evidencing the good biocompatibility of **R-TPE-LEC** FONs. When cells were excited with 543 nm laser, the cell uptake of **R-TPE-LEC** FONs can be clearly distinguished due to they were stained by **R-TPE-LEC** FONs. Furthermore, many dark areas, which were surrounded by **R-TPE-LEC** FONs areas could also be found from CLSM images. These dark areas are likely the location of cell nucleus. In the previous report,[22] amphiphilic block copolymers were employed to disperse hydrophobic organic dyes to form polymeric micelles, thus FONs were then carried out for intracellular imaging. Phagocytosis was believed as the possible mechanism for intracellular uptake by the cell, while the micelles could remain intact in the cells. In our work, phagocytosis may also be the possible mechanism for intracellular uptake by A549 cells, as compared with the size of FONs and nucleus pore (9×15 nm), these FONs are considered could not directly enter the cell nucleus. Therefore, we could expect that the **R-TPE-LEC** FONs should be promising candidates for various biomedical applications due to the combined advantages for bio-applications, such as unique PL properties, good water solubility, excellent biocompatibility, and biodegradable potential.

3. Conclusions

In summary, a novel strategy for fabrication of red FONs (**R-TPE-LEC**) was developed via mixing of a hydrophobic cyano-substituted

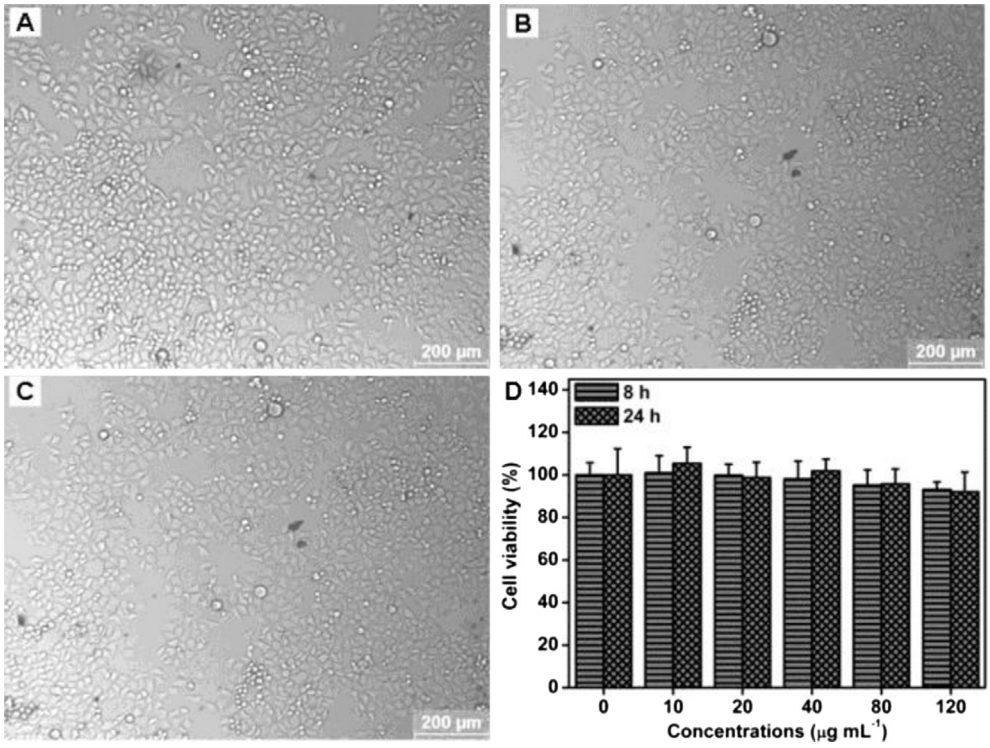

Fig. 4. Biocompatibility evaluation of **R-TPE-LEC** FONs. (A–C) Optical microscopy images of A549 cells incubated with different concentrations of **R-TPE-LEC** FONs for 24 h, (A) control cells, (B) 40 μg mL^{-1}, (C) 120 μg mL^{-1}, (D) cell viability of **R-TPE-LEC** FONs with A549 cells for 8 and 24 h, respectively. Cell viability was determined by the WST assay.

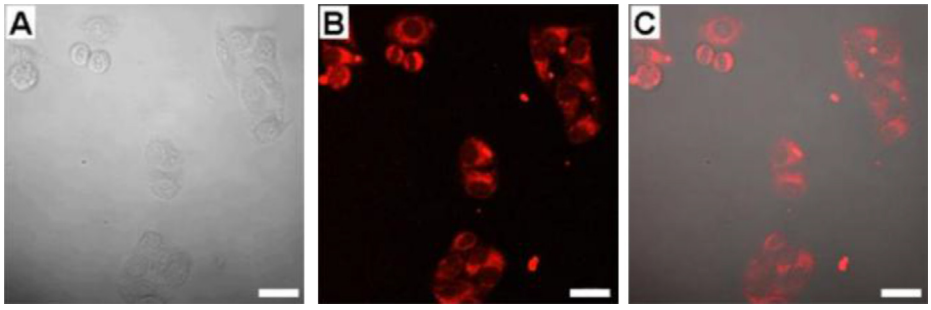

Fig. 5. CLSM images of A549 cells incubated with 100 μg mL^{-1} of **R-TPE-LEC** FONs for 3 h. (A) Bright field, (B) fluorescent image, which were excited with 543 nm laser, (C) merge images. Scale bar=20 μm.

diarylethylene and tetraphenylethene derivative conjugated molecule (**R-TPE**) and a commercial surfactant lecithin. Red FONs with diameter from 40 to 60 nm could be facilely obtained with uniform morphology and were subsequently utilized for cell imaging applications. Our results demonstrated that such red FONs show remarkable PL properties (anti-ACQ properties and broad excitation wavelength), excellent water solubility and biocompatibility, which are promising for bioimaging applications.

4. Experimental procedure

4.1. Materials and characterization

Thiophene, 3-(bromomethyl)heptane, thiophene-2-carboxylic acid, thionyl chloride, dimethylamine, *n*-butyllithium, stannic chloride, 1-bromo-1,2,2-triphenylethene, 4-(cyanomethyl)phenylboronic acid, toluene, Aliquat 336, potassium carbonate, tetrabutylammonium hydroxide (0.8 M in methanol) purchased from Alfa Aesar were used as received. All other agents and solvents were purchased from commercial sources and used directly without further purification. Ultra-pure water was used in the experiments.

^{1}H NMR and ^{13}C NMR spectra were measured on a JEOL 400 MHz spectrometer, $CDCl_3$ was used as solvent and tetramethylsilane (TMS) as the internal standard. HRMS was obtained on Shimadzu LCMS-IT-TOF high resolution mass spectrometry. Elemental analysis was performed with an Elementar Vario EL elemental analyzer. Fluorescence spectra were measured on a PE LS-55 spectrometer with a slit width of 3 nm for both excitation and emission. UV absorption spectra were recorded on an UV–vis–NIR Perkin–Elmer lambda750 spectrometer (Waltham, MA, USA) using quartz cuvettes of 1 cm path length. Transmission electron microscopy (TEM) images were recorded on a JEM-1200EX microscope operated at 100 kV, the TEM specimens were made by placing a drop of the nanoparticles suspension on a carbon-coated copper grid. The size distribution of **R-TPE-LEC** FONs in pure water was determined using a zeta Plus apparatus (ZetaPlus, Brookhaven Instruments, Holtsville, NY). The FT-IR spectra were obtained in a transmission mode on a Perkin–Elmer Spectrum 100 spectrometer (Waltham, MA, USA). Typically, eight scans at a resolution of 1 cm^{-1} were accumulated to obtain one spectrum.

4.2. Synthesis of R-TPE

The intermediate **2** were prepared according to the literature methods.[31] The synthetic route of **R-TPE** is showed in Scheme 1.

1-Bromo-1,2,2-triphenylethene (1.74 g, 5.2 mmol) and 4-(cyanomethyl)phenylboronic acid (1.00 g, 6.2 mmol) were dissolved in the mixture of toluene (40 mL), Aliquat 336 (10 drops), and 2 M potassium carbonate aqueous solution (10 mL). The mixture was stirred at room temperature for 0.5 h under Ar gas followed adding $Pd(PPh_3)_4$ (0.010 g, 8.70×10^{-3} mmol) and then heated to 90 °C for 24 h. After that the mixture was poured into water and extracted three times with ethyl acetate. The organic layer was dried over anhydrous sodium sulfate. After removing the solvent under reduced pressure, the residue was chromatographed on a silica gel column with petroleum ether/CH_2Cl_2 (3:1 by volume) as eluent to give intermediate **1** (1.30 g, 68% yield). ^{1}H NMR (400 MHz, $CDCl_3$) δ (ppm): 3.65 (s, 2H, $-CH_2-$), 6.98–7.06 (m, 10H, phenyl-H), 7.07–7.15 (m, 9H, phenyl-H); HRMS calcd for $C_{28}H_{21}N$ $[M+H]^+$: 372.1752, found 372.1759. Elemental analysis calcd for $C_{28}H_{21}N$: C, 90.53; H, 5.70; N, 3.77. Found: C, 90.37; H, 5.81; N, 3.69.

A solution of **2** (0.10 g, 0.16 mmol) and **1** (0.16 g, 0.43 mmol) in ethanol (10 mL) was stirred at room temperature. Then terabutyl ammonium hydroxide solution (0.8 M, five drops) was added and the mixture was heated to reflux for 2 h precipitating a dark red solid. The reaction mixture was cooled to room temperature and filtered, washed with ethanol for several times obtaining a dark red solid **R-TPE** (0.17 g, yield 80%). ^{1}H NMR (400 MHz, $CDCl_3$) δ (ppm): 0.88–0.99 (m, 12H, $-CH_3$), 1.30–1.48 (m, 16H, $-CH_2-$), 1.63–1.75 (m, 2H, (methylene)$_3$C–H), 2.86 (d, 4H, J=6.8 Hz, aryl–CH_2-), 6.92 (d, 2H, J=3.2 Hz, aryl-H), 6.97–7.20 (m, 34H, aryl-H), 7.34 (d, 2H, J=3.6 Hz, aryl-H), 7.39 (d, 4H, J=8.4 Hz, aryl-H), 7.62 (s, 2H, aryl-H), 8.02 (s, 2H, aryl-H); ^{13}C NMR (100 MHz, $CDCl_3$) δ (ppm): 146.83, 145.38, 143.47, 143.43, 143.29, 142.22, 140.26, 139.91, 139.68, 137.05, 135.77, 134.03, 132.20, 131.72, 131.46, 131.40, 131.38, 130.59, 128.01, 127.93, 127.79, 126.96, 126.82, 126.77, 125.94, 125.28, 124.94, 117.55, 110.96, 41.47, 34.36, 32.57, 28.99, 25.73, 23.14, 14.32, 10.97; HRMS calcd for $C_{92}H_{80}N_2S_4$ $[M+H]^+$: 1341.5283, found 1341.5243. Elemental analysis calcd for $C_{92}H_{80}N_2S_4$: C, 82.35; H, 6.01; N, 2.09; S, 9.56. Found: C, 82.59; H, 6.12; N, 2.01; S, 9.26.

4.3. Preparation of R-TPE-LEC FONs

The preparation of **R-TPE-LEC** FONs was carried out as follows. Approximately 10 mg of synthesized dyes (**R-TPE**) was dissolved in 20 mL of THF and then added dropwise under sonication into the solution of lecithin (50 mg) in 20 mL of H_2O in a 100 mL vial. And then the mixture was evaporated to completely remove the organic agent (THF) on a rotary evaporator at 40 °C. To remove the excess lecithin, the **R-TPE-LEC** water dispersion was treated by repeated centrifugal washing process for three times (centrifuged for 5 min at a rotational speed of 10,000 r/min).

4.4. Cytotoxicity of R-TPE-LEC FONs

Cell morphology was observed to examine the effects of **R-TPE-LEC** FONs to A549 cells. Briefly, cells were seeded in 6-well microplates at a density of 1×10^5 cells mL^{-1} in 2 mL of respective

media containing 10% FBS. After cell attachment, plates were washed with PBS and the cells were treated with complete cell culture medium, or different concentrations of fluoridated **R-TPE-LEC** FONs prepared in 10% FBS containing media for 24 h. Then all samples were washed with PBS three times to remove the uninternalized FONs. The morphology of cells was observed using an optical microscopy (Leica, Germany), the overall magnification was ×100.

The cell viability of **R-TPE-LEC** FONs on A549 cells was evaluated by cell counting kit-8 (CCK-8) assay. Briefly, cells were seeded in 96-well microplates at a density of 5×10^4 cells mL^{-1} in 160 μL of respective media containing 10% FBS. After 24 h of cell attachment, the cells were incubated with 10, 20, 40, 80, 120 μg mL^{-1} **R-TPE-LEC** FONs for 8 and 24 h. Then nanoparticles were removed and cells were washed with PBS three times. 10 μL of CCK-8 dye and 100 μL of DMEM cell culture medium were added to each well and incubated for 2 h at 37 °C. Plates were then analyzed with a microplate reader (VictorIII, Perkin–Elmer). Measurements of formazan dye absorbance were carried out at 450 nm, with the reference wavelength at 620 nm. The values were proportional to the number of live cells. The percent reduction of CCK-8 dye was compared to controls (cells not exposure to **R-TPE-LEC** FONs), which represented 100% CCK-8 reduction. Three replicate wells were used per microplate, and the experiment was repeated three times. Cell survival was expressed as absorbance relative to that of untreated controls. Results are presented as mean±standard deviation (SD).

4.5. Confocal microscopic imaging of cells using R-TPE-LEC FONs

A549 cells were cultured in Dulbecco's modified eagle medium (DMEM) supplemented with 10% heat-inactivated fetal bovine serum (FBS), 2 mM glutamine, 100 U mL^{-1} penicillin, and 100 μg mL^{-1} of streptomycin. Cell culture was maintained at 37 °C in a humidified condition of 95% air and 5% CO_2 in culture medium. Culture medium was changed every three days for maintaining the exponential growth of the cells. On the day prior to treatment, cells were seeded in a glass bottom dish with a density of 1×10^5 cells per dish. On the day of treatment, the cells were incubated with **R-TPE-LEC** FONs at a final concentration of 100 μg mL^{-1} for 3 h at 37 °C. Afterward, the cells were washed three times with PBS to remove the **R-TPE-LEC** FONs and then fixed with 4% paraformaldehyde for 10 min at room temperature. Cell images were taken with a Laser Scanning Confocal Microscope (LCSM) Zesis 710 3-channel (Zesis, Germany) with the excitation wavelengths of 543 nm.

Acknowledgements

This research was supported by the National Natural Science Foundation of China (Nos. 21134004, 21201108), and the National 973 Project (No. 2011CB935700), China Postdoctoral Science Foundation (2012M520243, 2013T60100).

References and notes

1. Weissleder, R.; Pittet, M. J. *Nature* **2008**, *452*, 580–589.
2. Lee, S.; Cha, E. J.; Park, K.; Lee, S. Y.; Hong, J. K.; Sun, I. C.; Kim, S. Y.; Choi, K.; Kwon, I. C.; Kim, K. *Angew. Chem., Int. Ed.* **2008**, *120*, 2846–2849.
3. Li, L.; Daou, T. J.; Texier, I.; Kim Chi, T. T.; Liem, N. Q.; Reiss, P. *Chem. Mater.* **2009**, *21*, 2422–2429.
4. Wang, F.; Banerjee, D.; Liu, Y.; Chen, X.; Liu, X. *Analyst* **2010**, *135*, 1839–1854.
5. Zhang, X.; Hui, J.; Yang, B.; Yang, Y.; Fan, D.; Liu, M.; Tao, L.; Wei, Y. *Polym. Chem.* **2013**, *4*, 4120–4125.
6. Lin, H. H.; Chan, Y. C.; Chen, J. W.; Chang, C. C. *J. Mater. Chem.* **2011**, *21*, 3170–3177.
7. Shu, X.; Royant, A.; Lin, M. Z.; Aguilera, T. A.; Lev-Ram, V.; Steinbach, P. A.; Tsien, R. Y. *Science* **2009**, *324*, 804–807.
8. Michalet, X.; Pinaud, F.; Bentolila, L.; Tsay, J.; Doose, S.; Li, J.; Sundaresan, G.; Wu, A.; Gambhir, S.; Weiss, S. *Science* **2005**, *307*, 538–544.
9. Frangioni, J. V. *Curr. Opin. Chem. Biol.* **2003**, *7*, 626–634.
10. Chandra, S.; Das, P.; Bag, S.; Laha, D.; Pramanik, P. *Nanoscale* **2011**, *3*, 1533–1540.
11. Díez, I.; Ras, R. H. A. *Nanoscale* **2011**, *3*, 1963–1970.
12. Wu, X.; He, X.; Wang, K.; Xie, C.; Zhou, B.; Qing, Z. *Nanoscale* **2010**, *2*, 2244–2249.
13. Zhang, X.; Wang, S.; Zhu, C.; Liu, M.; Ji, Y.; Feng, L.; Tao, L.; Wei, Y. *J. Colloid Interface Sci.* **2013**, *397*, 39–44.
14. Resch-Genger, U.; Grabolle, M.; Cavaliere-Jaricot, S.; Nitschke, R.; Nann, T. *Nat. Methods* **2008**, *5*, 763–775.
15. Cai, Z.; Ye, Z.; Yang, X.; Chang, Y.; Wang, H.; Liu, Y.; Cao, A. *Nanoscale* **2011**, *3*, 1974–1976.
16. Bhirde, A.; Xie, J.; Swierczewska, M.; Chen, X. *Nanoscale* **2011**, *3*, 142–153.
17. Smith, A. M.; Duan, H.; Mohs, A. M.; Nie, S. *Adv. Drug Delivery Rev.* **2008**, *60*, 1226–1240.
18. Wang, X.; Xu, S.; Xu, W. *Nanoscale* **2011**, *3*, 4670–4675.
19. Zhang, X.; Zhang, X.; Wang, S.; Liu, M.; Zhang, Y.; Tao, L.; Wei, Y. *ACS Appl. Mater. Interfaces* **2013**, *5*, 1943–1947.
20. Li, K.; Pan, J.; Feng, S. S.; Wu, A. W.; Pu, K. Y.; Liu, Y.; Liu, B. *Adv. Funct. Mater.* **2009**, *19*, 3535–3542.
21. Lin, H. H.; Su, S. Y.; Chang, C. C. *Org. Biomol. Chem.* **2009**, *7*, 2036–2039.
22. Wu, W.-C.; Chen, C.-Y.; Tian, Y.; Jang, S.-H.; Hong, Y.; Liu, Y.; Hu, R.; Tang, B. Z.; Lee, Y.-T.; Chen, C.-T.; Chen, W.-C.; Jen, A. K. Y. *Adv. Funct. Mater.* **2010**, *20*, 1413–1423.
23. An, B. K.; Gihm, S. H.; Chung, J. W.; Park, C. R.; Kwon, S. K.; Park, S. Y. *J. Am. Chem. Soc.* **2009**, *131*, 3950–3957.
24. Kumar, M.; George, S. J. *Nanoscale* **2011**, *3*, 2130–2133.
25. Zhang, X.; Chi, Z.; Yang, Z.; Chen, M.; Xu, B.; Zhou, L.; Wang, C.; Zhang, Y.; Liu, S.; Xu, J. *Opt. Mater.* **2009**, *32*, 94–98.
26. Thomas, S. W. I.; Joly, G. D.; Swager, T. M. *Chem. Rev.* **2007**, *107*, 1339–1386.
27. Pu, K. Y.; Li, K.; Shi, J.; Liu, B. *Chem. Mater.* **2009**, *21*, 3816–3822.
28. Zhang, X.; Wang, S.; Xu, L.; Ji, Y.; Feng, L.; Tao, L.; Li, S.; Wei, Y. *Nanoscale* **2012**, *4*, 5581–5584.
29. Liu, J.; Ding, D.; Geng, J.; Liu, B. *Polym. Chem.* **2012**, *3*, 1567–1575.
30. Zhang, X.; Zhang, X.; Wang, S.; Liu, M.; Tao, L.; Wei, Y. *Nanoscale* **2013**, *5*, 147–150.
31. Zhang, X.; Zhang, X.; Yang, B.; Liu, M.; Liu, W.; Chen, Y.; Wei, Y. *Polym. Chem.* **2013**, *4*, 4317–4321.
32. İbrahimova, V.; Ekiz, S.; Gezici, Ö.; Tuncel, D. *Polym. Chem.* **2012**, *2*, 2818–2824.
33. Zhang, X.; Zhang, X.; Yang, B.; Wang, S.; Liu, M.; Zhang, Y.; Tao, L.; Wei, Y. *RSC Adv.* **2013**, *3*, 9633–9636.
34. Zhang, X.; Liu, M.; Yang, B.; Zhang, X.; Wei, Y. *Colloids Surf., B* **2013**, *112*, 81–86.
35. Zhang, X.; Liu, M.; Yang, B.; Zhang, X.; Chi, Z.; Liu, S.; Xu, J.; Wei, Y. *Polym. Chem.* **2013**, *4*, 5060–5064.
36. Chen, M.; Yin, M. *Prog. Polym. Sci.* **2014**, *39*, 365–395.
37. Zhang, X.; Zhang, X.; Yang, B.; Zhang, Y.; Wei, Y. *ACS Appl. Mater. Interfaces* **2014**, *6*, 3600–3606.
38. Luo, J.; Xie, Z.; Lam, J. W. Y.; Cheng, L.; Chen, H.; Qiu, C.; Kwok, H. S.; Zhan, X.; Liu, Y.; Zhu, D.; Tang, B. Z. *Chem. Commun.* **2001**, 1740–1741.
39. An, B. K.; Kwon, S. K.; Jung, S. D.; Park, S. Y. *J. Am. Chem. Soc.* **2002**, *124*, 14410–14415.
40. Zhang, X.; Zhang, X.; Yang, B.; Hui, J.; Liu, M.; Liu, W.; Chen, Y.; Wei, Y. *Polym. Chem.* **2014**, *5*, 689–693.
41. Zhang, X.; Zhang, X.; Yang, B.; Liu, M.; Liu, W.; Chen, Y.; Wei, Y. *Polym. Chem.* **2014**, *5*, 399–404.
42. Zhang, X.; Zhang, X.; Yang, B.; Liu, M.; Liu, W.; Chen, Y.; Wei, Y. *Polym. Chem.* **2014**, *5*, 356–360.
43. Zhang, X.; Ma, Z.; Liu, M.; Zhang, X.; Jia, X.; Wei, Y. *Tetrahedron* **2013**, *69*, 10552–10557.
44. Zhang, X.; Chi, Z.; Li, H.; Xu, B.; Li, X.; Zhou, W.; Liu, S.; Zhang, Y.; Xu, J. *Chem.—Asian J.* **2011**, *6*, 808–811.
45. Zhang, X.; Chi, Z.; Li, H.; Xu, B.; Li, X.; Liu, S.; Zhang, Y.; Xu, J. *J. Mater. Chem.* **2011**, *21*, 1788–1796.
46. Zhang, X.; Chi, Z.; Zhang, Y.; Liu, S.; Xu, J. *J. Mater. Chem. C* **2013**, *1*, 3376–3390.
47. Li, X.; Zhang, X.; Chi, Z.; Chao, X.; Zhou, X.; Zhang, Y.; Liu, S.; Xu, J. *Anal. Methods* **2012**, *4*, 3338–3343.
48. Zhou, X.; Li, H.; Chi, Z.; Zhang, X.; Zhang, J.; Xu, B.; Zhang, Y.; Liu, S.; Xu, J. *New J. Chem.* **2012**, *36*, 685–693.
49. Zhang, X.; Yang, Z.; Chi, Z.; Chen, M.; Xu, B.; Wang, C.; Liu, S.; Zhang, Y.; Xu, J. *J. Mater. Chem.* **2009**, *20*, 292–298.
50. Zhang, X.; Chi, Z.; Xu, B.; Li, H.; Yang, Z.; Li, X.; Liu, S.; Zhang, Y.; Xu, J. *Dyes Pigm.* **2011**, *89*, 56–62.
51. Zhang, X.; Chi, Z.; Xu, B.; Li, H.; Zhou, W.; Li, X.; Zhang, Y.; Liu, S.; Xu, J. *J. Fluoresc.* **2011**, *21*, 133–140.
52. Yu, Y.; Feng, C.; Hong, Y.; Liu, J.; Chen, S.; Ng, K. M.; Luo, K. Q.; Tang, B. Z. *Adv. Mater.* **2011**, *23*, 3298–3302.
53. Chen, C.; Liao, J.-Y.; Chi, Z.; Xu, B.; Zhang, X.; Kuang, D.-B.; Zhang, Y.; Liu, S.; Xu, J. *RSC Adv.* **2012**, *2*, 7788–7797.
54. Chen, C.; Liao, J.-Y.; Chi, Z.; Xu, B.; Zhang, X.; Kuang, D.-B.; Zhang, Y.; Liu, S.; Xu, J. *J. Mater. Chem.* **2012**, *22*, 8994–9005.
55. Zhang, X.; Chi, Z.; Xu, B.; Chen, C.; Zhou, X.; Zhang, Y.; Liu, S.; Xu, J. *J. Mater. Chem.* **2012**, *22*, 18505–18513.
56. Zhang, X.; Chi, Z.; Zhang, J.; Li, H.; Xu, B.; Li, X.; Liu, S.; Zhang, Y.; Xu, J. *J. Phys. Chem. B* **2011**, *115*, 7606–7611.
57. Zhang, X.; Chi, Z.; Zhou, X.; Liu, S.; Zhang, Y.; Xu, J. *J. Phys. Chem. C* **2012**, *116*, 23629–23638.

58. Chi, Z.; Zhang, X.; Xu, B.; Zhou, X.; Ma, C.; Zhang, Y.; Liu, S.; Xu, J. *Chem. Soc. Rev.* **2012**, *41*, 3878–3896.
59. Zhang, X.; Ma, Z.; Yang, Y.; Zhang, X.; Chi, Z.; Liu, S.; Xu, J.; Jia, X.; Wei, Y. *Tetrahedron* **2014**, *70*, 924–929.
60. Zhang, X.; Zhang, X.; Yang, B.; Hui, J.; Liu, M.; Chi, Z.; Liu, S.; Xu, J.; Wei, Y. *J. Mater. Chem. C* **2014**, *2*, 816–820.
61. Zhang, X.; Zhang, X.; Yang, B.; Hui, J.; Liu, M.; Chi, Z.; Liu, S.; Xu, J.; Wei, Y. *Polym. Chem.* **2014**, *5*, 318–322.
62. Zhang, X.; Zhang, X.; Yang, B.; Hui, J.; Liu, M.; Chi, Z.; Liu, S.; Xu, J.; Wei, Y. *Polym. Chem.* **2014**, *5*, 683–688.
63. Zhang, X.; Hu, W.; Li, J.; Tao, L.; Wei, Y. *Toxicol. Res.* **2012**, *1*, 62–68.